# UC Irvine
## UC Irvine Previously Published Works

### Title
Stable ellipticity-induced Alfvén eigenmodes in the Joint European Torus

### Permalink
https://escholarship.org/uc/item/4594b8n4

### Journal
Physics of Plasmas, 4(10)

### ISSN
1070-664X

### Authors
Heidbrink, WW
Fasoli, A
Borba, D
et al.

### Publication Date
1997-10-01

### DOI
10.1063/1.872262

### Copyright Information
This work is made available under the terms of a Creative Commons Attribution License, availalbe at https://creativecommons.org/licenses/by/4.0/

Peer reviewed

eScholarship.org Powered by the California Digital Library
University of California

# Stable ellipticity-induced Alfvén eigenmodes in the Joint European Torus

W. W. Heidbrink
*University of California, Irvine, California 92697-4575*

A. Fasoli
*Joint European Torus Joint Undertaking, Abingdon, Oxfordshire, United Kingdom, and Centre de Recherches en Physique des Plasmas, Association EURATOM-Confédération Suisse*

D. Borba
*Joint European Torus Joint Undertaking, Abingdon, Oxfordshire, United Kingdom*

A. Jaun
*Alfvén Laboratory, Royal Institute of Technology, Stockholm, Sweden*

(Received 28 March 1997; accepted 8 July 1997)

An external antenna excites stable eigenmodes in elongated Ohmically heated plasmas in the Joint European Torus (JET) [P.-H. Rebut, R. J. Bickerton, and B. E. Keen, Nucl. Fusion **25**, 1011 (1985)]. The frequency of the modes (240−290 kHz) falls in the gap in the magnetohydrodynamic (MHD) continuum that is produced by ellipticity. Some modes are very weakly damped ($\gamma/\omega<10^{-3}$).
© *1997 American Institute of Physics.* [S1070-664X(97)01210-X]

## I. INTRODUCTION

In a cylinder, the spectrum of Alfvén waves is continuous in the ideal magnetohydrodynamic (MHD) model. In tokamaks, departures from cylindrical symmetry create gaps in the continuum. MHD theory predicts Alfvén eigenmodes (AE) in the gaps produced by beta (BAE),[1] toroidicity (TAE),[2] and ellipticity (EAE).[3] Unstable modes with frequencies similar to the expected BAE[4] and TAE[4,5] frequencies were first observed during neutral-beam heating. A possible EAE driven by beam ions was also reported.[1] In recent months, tail ions that are accelerated by ion cyclotron waves have destabilized EAE in the Joint European Torus (JET) and in the Japan Atomic Energy Research Institute Tokamak-60 Upgrade (JT-60U).[6]

Measurements of unstable, fast-ion driven instabilities are complemented by studies of stable modes. In JET, an external antenna excited stable TAE[7] and kinetic AE.[8] The first observation of stable EAE was also briefly reported.[9] This paper further documents the identification of the mode as an EAE. In addition, the first systematic measurements of the damping rate are presented and initial comparisons with theoretical models are given.

## II. EXPERIMENT

The modes are excited by passing ~5 A through two saddle coils on the bottom of JET.[9] For the experiments reported here, the antenna phasing is adjusted to excite predominantly modes with toroidal mode numbers $n$ of $\pm 2$. The excitation frequency is swept (typically between 150 and 300 kHz) and the driven response of the plasma is extracted from background noise using a set of synchronous detectors that provide the real and imaginary components of the signal. For these experiments, data from twelve electron cyclotron emission (ECE) radiometer signals,[10] four ordinary-mode reflectometer signals,[11] and a toroidal array of nine magnetic probes are archived.

The detector response to the antenna current can be described as a transfer function $H(\omega)$. An EAE resonance in the transfer function is shown in Fig. 1, corresponding to a mode at the frequency of 262 kHz. In the complex plane, the magnetic probe signal encircles the pole at $p=i\omega_0+\gamma$, where $\omega_0=2\pi f_{exp}$ is the (real) resonant frequency and $\gamma$ is the (imaginary) damping rate. The data from a complete set of diagnostic signals $\{x_i\}$ are analyzed by simultaneously fitting the measured transfer functions $H(\omega,x_i)$ to a rational fraction, $H=B/A$, where $B$ and $A$ are complex polynomials.[9] The denominator $A$ is assumed the same for all the signals and determines the characteristics of the resonance. Here $A$ is chosen to be of the second order to describe a single resonance. The numerators $B(\omega,x_i)$ (chosen of 5th order in this case to account for direct coupling between the antenna and the detectors) are proportional to the strength of the response. In particular, for the ECE measurements, the residues $B$ are related to the wave amplitude as a function of space, i.e., the radial eigenfunction. For the measurements presented here, the ECE and reflectometer signals are relatively weak, so the magnetic probe data govern the determination of $f_{exp}$ and $\gamma$.

Measurements from 42 resonances in Ohmically-heated limiter plasmas are entered into a database. The plasma parameters span the following conditions: toroidal field $B_T=2.1-3.1$ T, plasma current $I_p=1.5-2.6$ MA, edge safety factor $q_{95}=2.9-3.8$, major radius $R=2.9-3.0$ m, minor radius $a=0.85-1.03$ m, elongation $\kappa=1.31-1.72$, triangularity $\delta=0.01-0.16$, central electron density $n_e(0)=2.0-4.4\times10^{19}$ m$^{-3}$, and central electron temperature $T_e(0)=1.6-2.5$ keV.

Determination of the MHD gap structure requires knowledge of the profiles of safety factor $q$ and mass density $\rho$. The $q$ profile is calculated by the equilibrium reconstruction code EFIT,[12] using magnetics data and the sawtooth inversion radius (from ECE) as input to the code. The mass density is inferred from measurements of the electron density by six interferometer chords[13] and by Thomson scattering;[14]

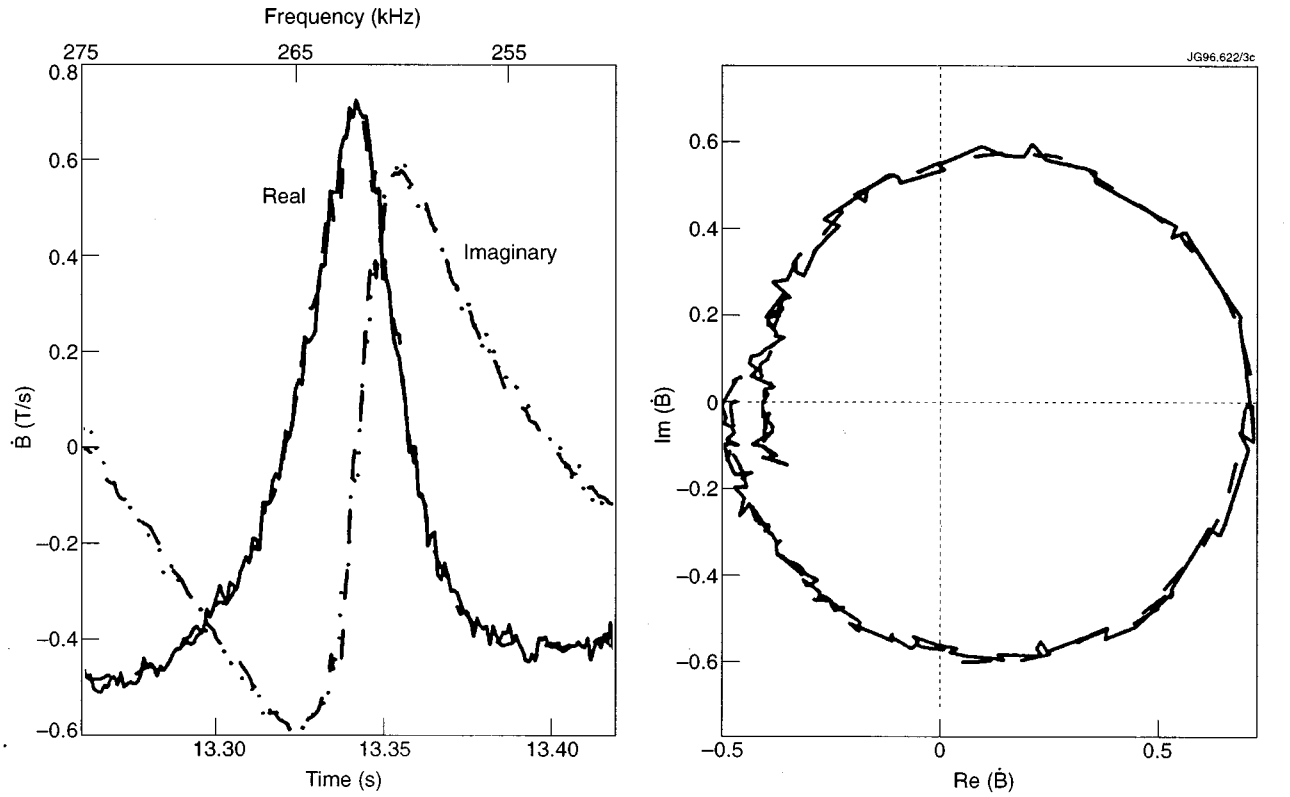


FIG. 1. In-phase and quadrature components of the signal from a magnetic probe as a function of time and frequency. (The frequency is swept linearly from 275 to 252 kHz.) The path of the signal in the complex plane is also shown. The dashed lines show the fit to the data from the nine magnetic probes: $f_{exp}=262.2$ kHz and $\gamma/\omega=9.5\times10^{-3}$. The statistical errors in the fit[9] are small compared to systematic errors associated with the selection of frequency windows (or the inclusion or deletion of a detector), which introduce uncertainties $\Delta f_{exp}\simeq0.2$ kHz and $\Delta\gamma/\omega\simeq0.5\times10^{-3}$ in this case. Plasma parameters: $R=2.94$ m, $a=1.03$ m, $\kappa=1.33$, $B_T=2.3$ T, $I_p=1.5$ MA, $T_e(0)=2.2$ keV, $n_e(0)=2.0\times10^{19}$ m$^{-3}$.

in these deuterium plasmas with few high-$Z$ impurities and little hydrogen the mass density is approximately $\rho\simeq2m_pn_e$, where $m_p$ is the proton mass. Systematic uncertainties in the data contribute more to the uncertainty in the calculated gap structure than random errors. At the plasma edge, the density inferred from interferometric measurements can differ by as much as 50% from Thomson scattering measurements, yielding a $\sim20\%$ variation in the predicted frequency. At the center, uncertainty in the $q$ profile typically generates $\sim10\%$ uncertainty in the continuum frequency. The uncertainty in the local magnetic shear is particularly large ($\sim50\%$ in the plasma interior). Corrections associated with the Doppler shift are negligible ($\sim1-2$ kHz).

The measured frequency $f_{exp}$ generally lies in the computed ellipticity-induced gap in the Alfvén continuum (Fig. 2). The center of the EAE gap occurs at a frequency of $f_{EAE}=v_A/2\pi qR$,[3] where $v_A$ is the Alfvén speed. In Fig. 3, all of the measurements of $f_{exp}$ are compared with $f_{EAE}$ at $s\simeq0.95$, $f_{edge}$. In 80% of the cases, the measured frequency lies in the computed EAE gap; in the remaining cases, $f_{exp}$ is from 1–9% higher than the calculated continuum at the upper edge of the EAE gap, but this is within the estimated uncertainty of the calculated value. The correlation of $f_{exp}$ with $f_{edge}$ ($r=0.53$) is stronger than the correlation with the EAE frequency at $s=0.5$, $f_{middle}$. Averaging over the data, the ratio $f_{exp}/f_{edge}=1.06\pm0.11$, while $f_{exp}/f_{middle}=0.78\pm0.10$. A profile-averaged EAE frequency, $\langle f_{EAE}\rangle=\langle v_A\rangle/2\pi(1.5)R$, only correlates weakly with $f_{exp}$. Apparently, the frequency of the mode excited by the antenna corresponds to the EAE frequency near the plasma edge.

On three frequency sweeps an eigenmode near $\sim150$ kHz is detected in addition to the eigenmode near 270 kHz

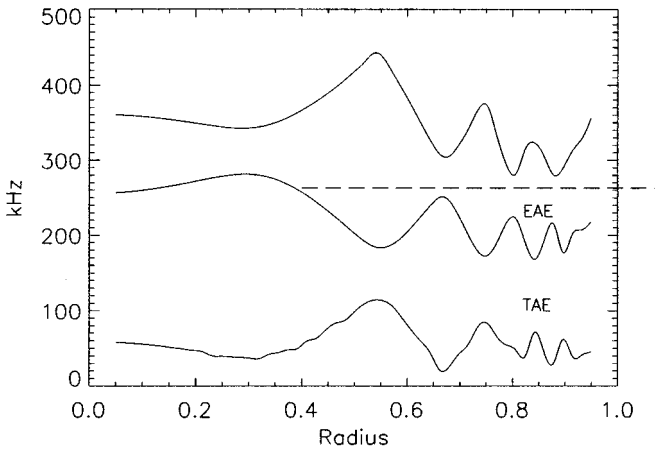


FIG. 2. The relationship of the resonance shown in Fig. 1 to the $n=2$ Alfvén continuum as calculated by the CSCAS code.[15] The frequency falls in the gap associated with ellipticity (EAE); the toroidicity-induced gap is also shown (TAE). The radial coordinate is the square root of the normalized poloidal flux $s=\sqrt{(\Psi-\Psi_0)/(\Psi_1-\Psi_0)}$.

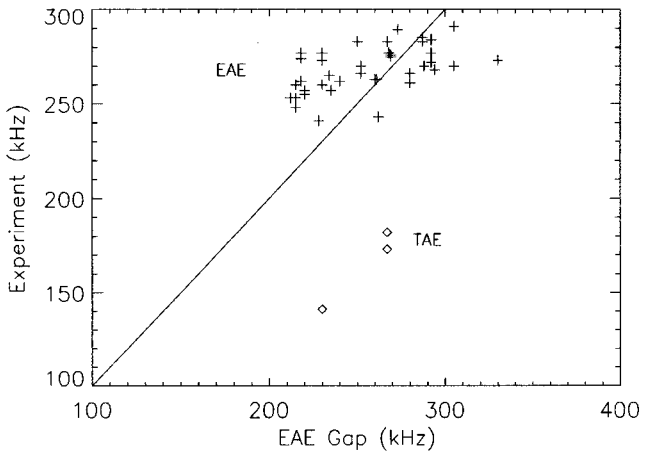


FIG. 3. Experimental resonant frequency $f_{exp}$ versus the center of the EAE gap at the plasma edge $f_{edge}$. On three frequency sweeps in the dataset, a low-frequency resonance was also detected ($\diamond$). The systematic error in $f_{edge}$ is possibly $\sim$20%; the uncertainty in $f_{exp}$ is negligible.

(Fig. 3). This lower-frequency mode falls in the gap created by toroidicity and is therefore identified as a TAE.[7]

Further confirmation that the observed resonances are global Alfvén eigenmodes is obtained from the ECE measurements (Fig. 4). Although the signals are too weak to obtain an accurate profile of the radial eigenfunction, the observation of measurable residues on several detectors confirms that the eigenfunction is globally extended, as expected for an EAE. For the case shown in Fig. 4, the ECE signal is largest where the frequency of the eigenmode intersects the $m=3$ Alfvén continuum in the middle of the plasma. Calculations of the expected eigenfunction with the CASTOR[16] and PENN[17] codes also predict a large amplitude near this intersection point (Fig. 4); however, the radius of the largest ECE signal does not coincide with the radius of the continuum crossing for all the modes in our EAE database.

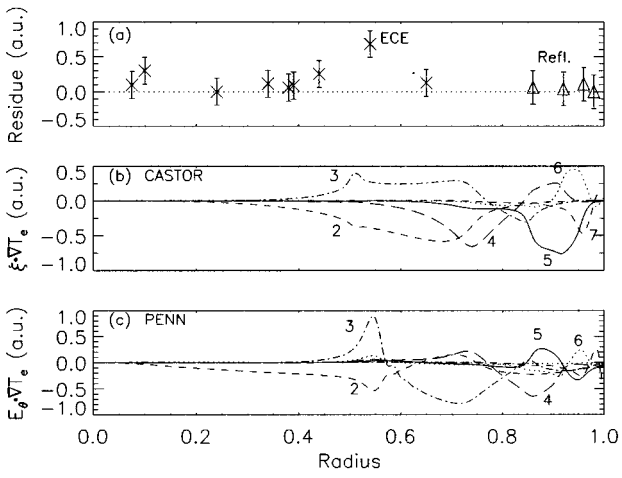


FIG. 4. Experimental and theoretical eigenfunctions for a discharge with $\kappa=1.54$, $B_T=3.0$ T, $I_p=2.5$ MA, $T_e(0)=2.0$ keV, and $n_e(0)=4.4\times10^{19}$ m$^{-3}$. (a) Amplitude versus radius $s$ for the ECE ($\times$) and O-mode reflectometer ($\triangle$) signals ($A\cos\phi$). The error bars are derived from the covariance matrix of the fitting routine.[9] (b) Poloidal decomposition of the radial magnetic field $\xi_\perp$ calculated by CASTOR.[16] The eigenfunction is multiplied by the derivative of the electron temperature since the expected ECE fluctuation is $\boldsymbol{\xi}\cdot\nabla T_e$. (c) Binormal electric field calculated by the kinetic version of PENN[17] multiplied by $\nabla T_e$. (The binormal component of $\mathbf{E}$ is approximately proportional to $\xi_\perp$.) In (b) and (c), only the largest amplitude harmonics are shown: $m=1$ (solid), 2 (dash), 3 (dash–dotted), 4 (long dash), 5 (solid), 6 (dot), 7 (dash).

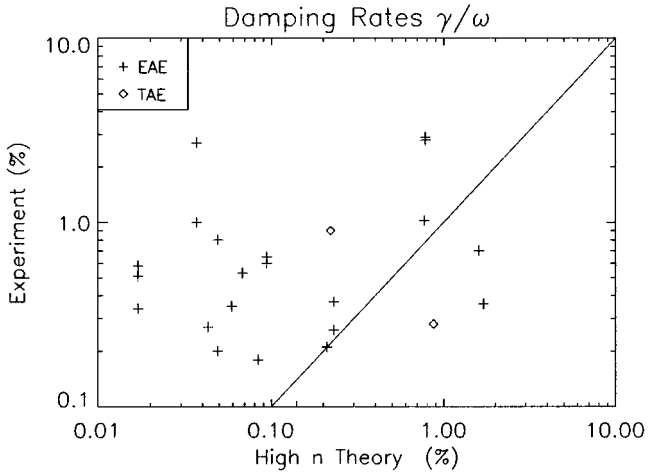


FIG. 5. Experimentally measured $\gamma/\omega$ for the EAE (+) and TAE ($\diamond$) versus the prediction of the single-gap theory of Ref. 18 (evaluated at the innermost open gap). The systematic uncertainties in the experimental measurement are typically 10%–20%, while large uncertainties in the theoretical predictions (a factor of 2–3) are associated with uncertainties in the magnetic shear and in the Alfvén gap structure.

The measured damping rates (Fig. 5) vary considerably, from values as low as $\gamma/\omega=8\times10^{-4}$ to values as large as 3%. The dependence of $\gamma/\omega$ on plasma parameters is complicated. Even during nominally steady-state conditions in the same discharge, $\gamma/\omega$ can double on successive frequency sweeps. For our dataset, the correlation of $\gamma/\omega$ with $v_A$, $n_e(0)$, $a$, $\kappa$, $\delta$, $q_{95}$, $I_p$, and $T_e$ is weak ($r^2<0.22$); the correlation with the magnetic shear at $s=0.50$, $s_{50}$, and with the shear at the edge, $s_{95}$, is also weak. For the weakly damped modes ($\gamma/\omega<1\%$), the strongest correlation in the dataset is with the toroidal field ($r=-0.72$). This dependence may reflect an underlying dependence of the damping rate on the gyroradius. [The correlation with $\sqrt{T_e(0)}/B^2$ is weaker, however.] No correlation with the nonideal parameter[18] $\lambda\propto s_{95}q_{95}\sqrt{T_e}/B_T$ is observed.

## III. THEORY

Possible EAE damping mechanisms include trapped electron collisional absorption,[19,20] continuum damping,[21,22] radiative damping,[18] and, more generally, Landau damping through mode conversion.[23] (Ion Landau damping[24] should be negligible in these Ohmically-heated discharges.) A formalism for calculating the expected damping rate associated with electron collisional and radiative damping in realistic geometry was developed by Mett *et al.*[18] The theory only treats the interaction of a single pair of poloidal harmonics. This ''high-$n$'' assumption is of dubious validity for the $n=2$ modes considered here,[25] although the theory did successfully predict the stability threshold of $n=4$ TAE modes in DIII-D (to within a factor of two).[18] We have applied this theory to our data. The frequencies at the top and bottom of

the gap $\omega_{top}$ and $\omega_{bottom}$ are obtained from the calculations of the gap structure. Two different radial locations are selected for this evaluation: near $s=0.95$ and at the gap adjacent to the interior continuum crossing (for example, for the case shown in Fig. 2, the continuum frequencies are measured at $s=0.66$). The results of this analysis are shown in Fig. 5 for the interior gaps. The results for $s=0.95$ are similar. Clearly, this simple theory cannot explain the observations. On the other hand, the predictions are of the right order of magnitude, so it is possible that electron collisional and radiative damping are important damping mechanisms.

Comparisons that properly treat the mode structure are computationally expensive, so only a single discharge with both an EAE and a TAE resonance is analyzed in this study. Initially, the PENN code[17] found eigenmodes at frequencies that are consistent with the experimental values, but the predicted damping of the EAE exceeded the experimental value ($\gamma/\omega=0.14\pm0.06\%$) by a factor of 5–10. A numerical convergence study performed *a posteriori* showed that higher numerical resolution was in fact required to represent correctly the mode coupling occurring in the plasma core ($s<0.2$); using a densified mesh with 96, 128, or 192 radial mesh points finally yielded a theoretically converged value ($0.26\pm0.04\%$) which is in acceptable agreement with the experimental measurement. Initial calculations with the CASTOR code[16] correctly predicted the frequency of the TAE, but the frequency of the computed EAE was only $\sim80\%$ of the experimental value. Judicious reduction of the density near the edge by 20% (which is within experimental uncertainties) yielded satisfactory agreement with the measured frequencies; however, the predicted damping ($\sim1\%$) still exceeded the experimental value. The CASTOR damping prediction is large because the computed EAE singularity occurs within a dominant poloidal harmonic. Further tailoring of the profile to shift the location of the singularity could yield a smaller damping rate.

## IV. CONCLUSION

Eigenmodes with frequencies that lie in the ellipticity-induced gap in the Alfvén continuum are observed in JET. The damping of these EAE span from $\gamma/\omega\lesssim10^{-3}$ to values $\lesssim0.1$, i.e., the same range as the TAE.[8] Although the predicted destabilizing term produced by energetic ions is a factor of two smaller for the EAE,[24] the measured damping rates vary by orders of magnitude, so the EAE could prove dangerous in a reactor. The damping seems to depend sensitively on subtle details of the plasma profiles, thus making stability projections problematic.

## ACKNOWLEDGMENTS

The assistance of S. Ali-Arshad, J. deHaas, H. Holties, G. Huysmans, P. Lavanchy, D. O'Brien, L. Porte, S. Sharapov, K. Thomsen, and the entire JET team is gratefully acknowledged. A computer code written by R. Mett was used for the comparison with the high- $n$ theory. The experiments and A. F. were partially supported by the *Fonds National Suisse pour la Recherche Scientifique* within a JET/Center de Recherches en Physique des Plasmas Task Agreement.

W. W. H. acknowledges support from Subcontract No. SC-L134501 to the U.S. Department of Energy Contract No. DE-AC03-89ER51114. A. J. was supported by the Swedish National Science Foundation and the supercomputer center in Linkoping.

[1] A. D. Turnbull, E. J. Strait, W. W. Heidbrink, M. S. Chu, H. H. Duong, J. M. Greene, L. L. Lao, T. S. Taylor, and S. J. Thompson, Phys. Fluids B **5**, 2546 (1993).
[2] C. Z. Cheng and M. S. Chance, Phys. Fluids **29**, 3695 (1986).
[3] R. Betti and J. P. Freidberg, Phys. Fluids B **3**, 1865 (1991).
[4] W. W. Heidbrink, E. J. Strait, M. S. Chu, and M. S. Turnbull, Phys. Rev. Lett. **71**, 855 (1993).
[5] K. L. Wong, R. J. Fonck, S. F. Paul, D. R. Roberts, E. D. Fredrickson, R. Nazikian, H. K. Park, M. Bell, N. L. Bretz, R. Budny, S. Cohen, G. W. Hammett, F. C. Jobes, D. M. Meade, S. S. Medley, D. Mueller, Y. Nagayama, D. K. Owens, and E. J. Synakowski, Phys. Rev. Lett. **66**, 1874 (1991).
[6] G. J. Kramer, M. Saigusa, T. Ozeki, Y. Kusama, H. Kimura, T. Oikawa, K. Tobita, G. Y. Fu, and C. Z. Cheng, ''Noncircular triangularity and ellipticity induced Alfvén eigenmodes observed in JT-60U,'' submitted to Phys. Rev. Lett.
[7] A. Fasoli, D. Borba, G. Bosia, D. J. Campbell, J. A. Dobbing, C. Gormezano, J. Jacquinot, P. Lavanchy, J. B. Lister, P. Marmillod, J.-M. Moret, A. Santagiustina, and S. Sharapov, Phys. Rev. Lett. **75**, 645 (1995).
[8] A. Fasoli, J. B. Lister, S. Sharapov, D. Borba, N. Deliyanakis, C. Gormezano, J. Jacquinot, A. Jaun, H. A. Holties, G. T. A. Huysmans, W. Kerner, J.-M. Moret, and L. Villard, Phys. Rev. Lett. **76**, 1067 (1996).
[9] A. Fasoli, J. B. Lister, S. Sharapov, S. Ali-Arshad, G. Bosia, D. Borba, D. J. Campbell, N. Deliyanakis, J. A. Dobbing, C. Gormezano, H. A. Holties, G. T. A. Huysmans, J. Jacquinot, A. Jaun, W. Kerner, P. Lavanchy, J.-M. Moret, L. Porte, A. Santagiustina, and L. Villard, Nucl. Fusion **35**, 1485 (1995).
[10] A. E. Costley, in *Diagnostics for Contemporary Fusion Experiments* (Editrice Compositori, Bologna, 1991), p. 223.
[11] A. C. C. Sips, A. L. Colton, A. E. Costley, G. J. Kramer, and R. Prentice, in *Diagnostics for Contemporary Fusion Experiments* (Editrice Compositori, Bologna, 1991), p. 755.
[12] L. L. Lao, H. St. John, R. D. Stambaugh, A. G. Kellman, and W. P. Pfeiffer, Nucl. Fusion **25**, 1611 (1985).
[13] G. Braithwaite, N. Gotlardi, G. Magyar, J. O'Rourke, J. Ryan, and D. Véron, Rev. Sci. Instrum. **60**, 2825 (1989).
[14] C. Gowers, in *Diagnostics for Contemporary Fusion Experiments* (Editrice Compositori, Bologna, 1991), p. 261.
[15] S. Poedts and E. Schwartz, J. Comput. Phys. **105**, 165 (1993).
[16] G. T. A. Huysmans, J. P. Goedbloed, and W. Kerner, Phys. Fluids B **5**, 1545 (1993).
[17] A. Jaun, K. Appert, J. Vaclavik, and L. Villard, Comput. Phys. Commun. **92**, 153 (1995).
[18] R. R. Mett, E. J. Strait, and S. M. Mahajan, Phys. Plasmas **1**, 3277 (1994).
[19] N. N. Gorelenkov and S. Sharapov, Phys. Scr. **45**, 163 (1992).
[20] J. Candy and M. N. Rosenbluth, Plasma Phys. Controlled Fusion **35**, 957 (1993).
[21] M. N. Rosenbluth, H. L. Berk, J. W. van Dam, and D. M. Lindberg, Phys. Rev. Lett. **68**, 596 (1992).
[22] F. Zonca and L. Chen, Phys. Rev. Lett. **68**, 592 (1992).
[23] A. Jaun, K. Appert, A. Fasoli, T. Hellsten, J. Lister, J. Vaclavik, and L. Villard, Plasma Phys. Controlled Fusion **39**, 549 (1997); A. Jaun, J. Vaclavik, and L. Villard, Phys. Plasmas **4**, 1110 (1997).
[24] R. Betti and J. P. Friedberg, Phys. Fluids B **4**, 1465 (1992).
[25] L. Villard, S. Brunner, and J. Vaclavik, Nucl. Fusion **35**, 1173 (1995).